JOC The Journal of Organic Chemistry

Featured Article

pubs.acs.org/joc

Identification and Characterization of Second-Generation Invader Locked Nucleic Acids (LNAs) for Mixed-Sequence Recognition of Double-Stranded DNA

Sujay P. Sau,[†] Andreas S. Madsen,[‡] Peter Podbevsek,[§] Nicolai K. Andersen,[‡] T. Santhosh Kumar,[‡] Sanne Andersen,[†,‡] Rie L. Rathje,[†,‡] Brooke A. Anderson,[†] Dale C. Guenther,[†] Saswata Karmakar,[†] Pawan Kumar,[†] Janez Plavec,[§] Jesper Wengel,[‡] and Patrick J. Hrdlicka*[,†]

[†]Department of Chemistry, University of Idaho, Moscow, Idaho 83844, United States

[‡]Nucleic Acid Center, Department of Physics and Chemistry, University of Southern Denmark, DK-5230 Odense M, Denmark

[§]National Institute of Chemistry, 1000 Ljubljana, Slovenia

Supporting Information

ABSTRACT: The development of synthetic agents that recognize double-stranded DNA (dsDNA) is a long-standing goal that is inspired by the promise for tools that detect, regulate, and modify genes. Progress has been made with triplex-forming oligonucleotides, peptide nucleic acids, and polyamides, but substantial efforts are currently devoted to the development of alternative strategies that overcome the limitations observed with the classic approaches. In 2005, we introduced Invader locked nucleic acids (LNAs), i.e., double-stranded probes that are activated for mixed-sequence recognition of dsDNA through modification with "+1 interstrand zippers" of 2′-*N*-(pyren-1-yl)methyl-2′-amino-α-L-LNA monomers. Despite promising preliminary results, progress has been slow because of the synthetic complexity of the building blocks. Here we describe a study that led to the identification of two simpler classes of Invader monomers. We compare the thermal denaturation characteristics of double-stranded probes featuring different interstrand zippers of pyrene-functionalized monomers based on 2′-amino-α-L-LNA, 2′-*N*-methyl-2′-amino-DNA, and RNA scaffolds. Insights from fluorescence spectroscopy, molecular modeling, and NMR spectroscopy are used to elucidate the structural factors that govern probe activation. We demonstrate that probes with +1 zippers of 2′-*O*-(pyren-1-yl)methyl-RNA or 2′-*N*-methyl-2′-*N*-(pyren-1-yl)methyl-2′-amino-DNA monomers recognize DNA hairpins with similar efficiency as original Invader LNAs. Access to synthetically simple monomers will accelerate the use of Invader-mediated dsDNA recognition for applications in molecular biology and nucleic acid diagnostics.

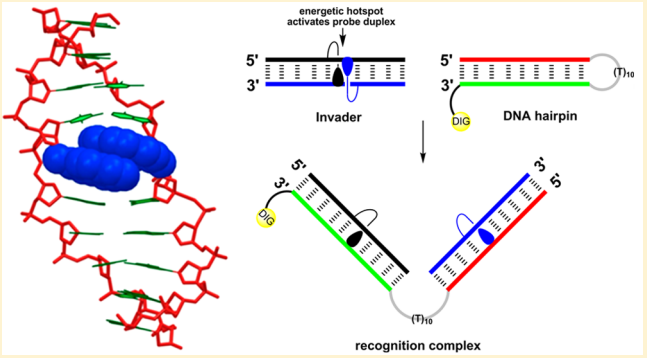

INTRODUCTION

The development of strategies for sequence-unrestricted targeting of double-stranded DNA (dsDNA) continues to be one of the great challenges of biological chemistry. Efforts are fueled by the promise for powerful molecular tools that enable gene regulation, modification, and detection and drug candidates against genetic diseases.[1−6] Significant progress toward this end has been made with triplex-forming oligonucleotides (TFOs), peptide nucleic acids (PNAs), and minor-groove-binding polyamides.[7−11] However, these pioneering dsDNA-targeting approaches display limitations that have restricted their widespread use. For example, TFOs and regular PNAs recognize only homopurine targets, most PNA-based approaches require nonphysiological salinity, and polyamides are typically used only against short target regions, which complicates recognition of unique targets in the genome. These drawbacks have spurred the development of alternative strategies for mixed-sequence recognition of dsDNA such as pseudocomplementary DNA (pcDNA),[12] pcPNA,[13,14] antigene PNA,[15] antigene locked nucleic acid (LNA),[16] γ-PNA,[17,18] TFOs with engineered nucleobases,[19,20] engineered proteins,[21,22] and other approaches.[23−28] Nonetheless, there remains a need for probes that enable rapid, potent, and specific targeting of mixed-sequence dsDNA under physiologically relevant conditions, which are inexpensive, compatible with delivery agents, and amenable to large-scale production.

In 2005, we introduced Invader LNAs as an alternative strategy for mixed-sequence dsDNA recognition.[29] Briefly described, Invader LNAs are double-stranded probes that are activated for dsDNA recognition through modification with one or more "+1 interstrand zippers" of 2′-*N*-(pyren-1-yl)methyl-2′-amino-α-L-LNA (**W**)

Received: July 23, 2013
Published: September 13, 2013

   dx.doi.org/10.1021/jo4015936 | J. Org. Chem. 2013, 78, 9560−9570

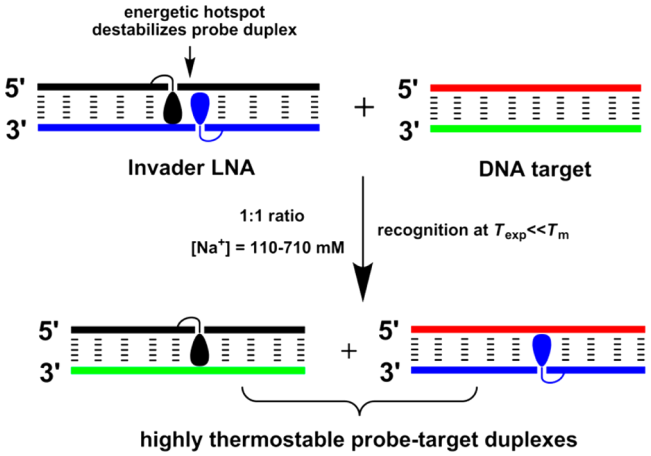

Figure 1. Illustration of the Invader approach for mixed-sequence recognition of dsDNA. Droplets denote intercalating pyrene moieties.

monomers (Figures 1 and 2; for a definition of the zipper nomenclature, see ref 30). This particular monomer arrangement results in duplex destabilization, presumably because the pyrene moieties are forced to intercalate into the same region, leading to excessive local duplex unwinding and the formation of "energetic hotspots" (Figure 1).[29,31] On the other hand, the two strands that constitute an Invader LNA display very strong affinity toward complementary single-stranded DNA (ssDNA) as a result of efficient pyrene intercalation and $\pi-\pi$ stacking with neighboring base pairs (Figure 1).[29,31,32] We have used the difference in the thermostabilities of Invader LNAs and probe–target duplexes to realize mixed-sequence recognition of short isosequential dsDNA targets (Figure 1).[29,31] For example, addition of a 13-mer Invader LNA with two energetic hotspots to equimolar quantities of an isosequential dsDNA target results in ~50% recognition within ~30 min (110 mM NaCl, pH 7, T_{exp} = 20 °C).[31] The recognition likely entails partial unwinding of the probe and/or target duplexes but does not appear to require full duplex dissociation.

A related dsDNA-targeting approach in which DNA duplexes with adjacent incorporations of intercalator-modified non-nucleotide monomers were used to inhibit in vitro transcription in cell-free assays appeared in the scientific literature[26] following our original studies.[29] NMR studies have shown that this approach relies on intercalator-mediated duplex unwinding for probe destabilization[33] in a similar manner as hypothesized for Invader LNAs.

In spite of the interesting initial results, progress with Invader LNAs has been slow, in large part because of the difficult synthesis of the corresponding phosphoramidite of monomer **W** (~3% yield from diacetone-α-D-glucose over ~20 steps).[32] A promise of synthetically more readily accessible Invader building blocks came when we discovered that oligodeoxyribonucleotides (ONs) modified with 2′-*O*-(pyren-1-yl)-methyluridine monomer **P** or 2′-*N*-methyl-2′-*N*-(pyren-1-yl)-methyl-2′-aminodeoxyuridine monomer **Q** (Figure 2) display similar affinities toward complementary DNA as **W**-modified ONs[34] since their pyrene moieties also are predisposed for intercalation into DNA duplexes.[34−36] Importantly, the corresponding phosphoramidites are obtained from uridine in only four and seven steps, respectively.[34] Indeed, we recently demonstrated that monomer **P** can be used in lieu of the original LNA-based building block **W** to generate second-generation Invaders that recognize chromosomal DNA in nondenaturing fluorescence in situ hybridization (nd-FISH) experiments, marking a proof of concept for Invader-mediated mixed-sequence recognition of biological dsDNA.[37] Invaders based on 2′-*O*-(pyren-1-yl)-methyl RNA monomers have also been used in sandwich assays to recognize linear dsDNA targets specific to foodborne pathogens.[38]

In the present article, we describe the process that resulted in the identification of the second-generation Invader building blocks **Q**, **P**, and **R**. At the onset of this study, we had the following goals: (i) to examine whether the thermal activation observed for double-stranded probes with +1 interstrand zippers of 2′-*N*-(pyren-1-yl)methyl-2′-amino-α-L-LNA T monomers is a unique property of **W** monomers or if it can be emulated or even optimized using other zipper arrangements and/or building blocks (Figure 2); (ii) to determine the structural factors that govern thermal activation of duplexes with certain interstrand zipper arrangements of pyrene-functionalized nucleotides; and (iii) to demonstrate Invader-mediated mixed-sequence recognition of challenging dsDNA targets.

RESULTS AND DISCUSSION

Synthesis of ONs. In the present study, we utilized a series of singly modified 9-mer ONs, the vast majority of which were prepared and characterized with respect to identity (MALDI-MS) and purity [>80%, ion-pair reversed-phase (RP) HPLC] in previous studies.[32,34,39,40] The synthesis and characterization of new ONs (**P3** and the **R** series) is described in the Experimental Section. ONs containing a single modification in the 5′-GBG ATA TGC context are denoted as **N1**, **O1**, **P1**, etc. Similar conventions apply for ONs in the **B2**–**B9** series (Tables 1 and 2).

Hybridization Characteristics of Pyrene-Functionalized ONs with ssDNA Targets. We have previously demonstrated that 9-mer ONs, which are singly modified with N2′-pyrene-functionalized 2′-amino-α-L-LNA thymine monomers **W**–**Z** (Figure 2) display greatly increased thermal affinities toward ssDNA relative to unmodified ONs (ΔT_m between +0.5 and +19.5 °C; Table 1).[32] The degree of duplex stabilization depends on the strength of the stacking interactions

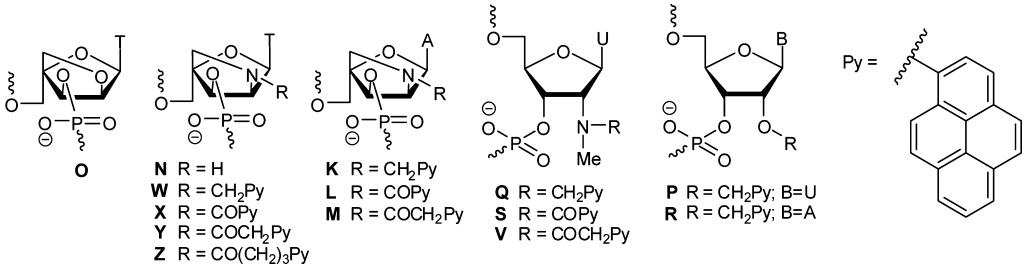

Figure 2. Structures of monomers studied herein.

dx.doi.org/10.1021/jo4015936 | J. Org. Chem. 2013, 78, 9560−9570

Table 1. ΔT_m Values of Duplexes between ONs Modified with Pyrene-Functionalized Thymine/Uracil Monomers and Complementary DNA, Measured Relative to Unmodified Duplexes[a]

			ΔT_m/°C									
ON	duplex	for **B** =	**O**[b]	**N**[b]	**W**[b]	**X**[b]	**Y**[b]	**Z**[b]	**Q**[c]	**S**[c]	**V**[c]	**P**[c]
B1	5′-G**B**G ATA TGC		+2.5	−2.0	+7.0	+10.0	+10.5	+0.5	+5.0	−6.0	−0.5	+5.0
D2	3′-CAC TAT ACG											
B2	5′-GTG A**B**A TGC		+6.0	+0.5	+14.0	+19.0	+15.5	+6.0	+14.0	+3.0	+6.0	+12.5
D2	3′-CAC TAT ACG											
B3	5′-GTG ATA **B**GC		+3.0	−1.0	+10.5	+14.0	+11.5	–	–	–	–	+8.0[d]
D2	3′-CAC TAT ACG											
D1	5′-GTG ATA TGC		+3.5	−0.5	+6.5	+10.5	+10.0	+0.5	+1.5	−6.0	+1.0	+3.5
B4	3′-CAC **B**AT ACG											
D1	5′-GTG ATA TGC		+8.0	+2.5	+15.5	+19.5	+16.5	+6.5	+13.0	+4.0	+6.5	+11.5
B5	3′-CAC TA**B** ACG											

[a]ΔT_m = change in T_m relative to the unmodified reference duplex **D1**:**D2** (T_m = 29.5 °C); T_m values were determined as the first-derivative maxima of denaturation curves (A_{260} vs T) recorded in medium-salt buffer ([Na^+] = 110 mM, [Cl^-] = 100 mM, pH 7.0 (NaH_2PO_4/Na_2HPO_4)), using a 1.0 μM concentration of each strand. T_m values are averages of at least two measurements within 1.0 °C; A = adenin-9-yl-DNA monomer, C = cytosin-1-yl-DNA monomer, G = guanin-9-yl-DNA monomer, T = thymin-1-yl-DNA monomer. See Figure 1 for structures of monomers. "–" = not determined. [b]Previously reported in ref 32. [c]Previously reported in ref 34. [d]Not previously reported.

Table 2. ΔT_m Values of Duplexes between ONs Modified with Pyrene-Functionalized Adenine Monomers and Complementary DNA, Measured Relative to Unmodified Duplexes[a]

			ΔT_m/°C			
ON	duplex	for **B** =	**K**[b]	**L**[b]	**M**	**R**
B6	5′-GTG **B**TA TGC		+5.0	+11.0	+6.0	+4.5
D2	3′-CAC TAT ACG					
B7	5′-GTG AT**B** TGC		+7.0	+14.0	+7.5	+8.5
D2	3′-CAC TAT ACG					
D1	5′-GTG ATA TGC		+6.5	+11.5	+7.5	+8.5
B8	3′-CAC T**B**T ACG					
D1	5′-GTG ATA TGC		+5.5	+12.0	+6.0	+6.5
B9	3′-CAC TAT **B**CG					

[a]ΔT_m = change in T_m value relative to the unmodified reference duplex **D1**:**D2** (T_m = 29.5 °C); see Table 1 for experimental conditions; see Figure 1 for structures of monomers. [b]Previously reported in ref 40.

between the intercalating pyrene and the flanking nucleobases. This, concomitantly, depends on the specific nature of the 3′-flanking nucleotide (purines induce greater stabilization than pyrimidines) and the linker between the pyrene moiety and the bicyclic sugar skeleton. Monomers with short linkers result in greater duplex stabilization than monomers with long linkers (trend: **X** > **Y** ≫ **Z**). Moreover, monomers in which the pyrene is attached via an acyl linker induce greater stabilization than monomers using alkyl linkers (trend: **X** > **W**). Similar trends were observed for ONs modified with the corresponding adenine monomers **K**/**L**/**M** (Figure 2 and Table 2).[40] In contrast, ONs that are singly modified with 2′-oxy-α-L-LNA thymine monomer **O** or nonfunctionalized 2′-amino-α-L-LNA thymine monomer **N** display more moderate affinities toward ssDNA (Figure 2 and Table 1),[32] which underscores the important stabilizing role of the pyrenes of monomers **W**–**Z**.

We recently demonstrated that ONs modified with *N*2′-pyrene-functionalized 2′-*N*-methyl-2′-aminodeoxyuridine monomers **Q**, **S**, and **V** (Figure 2) display highly linker-dependent variations in ssDNA affinity. With this compound class, alkyl linkers induce far greater ssDNA affinity than monomers with acyl linkers (ΔT_m varying from −6.0 to +14.0 °C, trend: **Q** ≫ **V** > **S**; Table 1).[34] Importantly, ONs modified with 2′-*N*-methyl-2′-*N*-(pyren-1-yl)methyl-2′-aminodeoxyuridine monomer **Q** or the closely related 2′-*O*-(pyren-1-yl)-methyluridine monomer **P** display similar ssDNA affinity as ONs modified with the original Invader building block **W** (Table 1).[34] An equivalent relationship was observed for ONs modified with adenine monomers **R** and **K** (Figure 2 and Table 2), supporting our hypothesis that certain *N*2′-pyrene-functionalized 2′-*N*-methyl-2′-amino-DNA and *O*2′-pyrene-functionalized RNA monomers are mimics of synthetically more elaborate *N*2′-pyrene-functionalized 2′-amino-α-L-LNA monomers.

Thermostability of Duplexes with Interstrand Arrangements of Pyrene-Functionalized Monomers. The thermostability of DNA duplexes with different interstrand zipper arrangements of pyrene-functionalized monomers was measured to identify monomers and probe architectures that are activated for dsDNA recognition via the Invader strategy (Table 3). The impact on duplex stability upon incorporation of a second monomer can be additive, cooperative (i.e., more than additive), or antagonistic (i.e., less than additive) relative to a corresponding singly modified duplex. This is readily estimated by the term "deviation from additivity" (DA) defined as: $DA_{ONX:ONY} \equiv \Delta T_m(\mathbf{ONX}:\mathbf{ONY}) - [\Delta T_m(\mathbf{ONX}:\text{ssDNA}) + \Delta T_m(\text{ssDNA}:\mathbf{ONY})]$, where **ONX**:**ONY** is a duplex with an interstrand monomer arrangement. Double-stranded probes with highly negative DA values are thermally activated for recognition of isosequential dsDNA via the process depicted in Figure 1, as this indicates that the probe–target duplexes are more thermostable than the Invader probe and dsDNA target.

As previously reported,[29] duplexes with +4 or −3 interstrand zippers of **W** monomers are (i) strongly stabilized relative to

dx.doi.org/10.1021/jo4015936 | J. Org. Chem. 2013, 78, 9560–9570

Table 3. ΔT_m and DA Values for DNA Duplexes with Different Interstrand Zipper Arrangements of Thymine/Uracil Monomers[a]

			ΔT_m/°C [DA/°C]									
ON	zipper	duplex	for **B** =	**O**	**N**	**W**[b]	**X**	**Y**	**Z**	**Q**	**S**	**V**	**P**
B1	+4	5′-G**B**G ATA TGC		+11.0 [+0.5]	+1.0 [+0.5]	+25.0 [+2.5]	+28.5 [−1.0]	+26.0 [−1.0]	+8.5 [+1.5]	+19.5 [+1.5]	−3.5 [−5.5]	+9.0 [+3.0]	+16.5 [0.0]
B5		3′-CAC TA**B** ACG											
B1	+2	5′-G**B**G ATA TGC		+8.0 [+2.0]	−1.5 [+1.0]	0.0 [−13.5]	+6.5 [−14.0]	+12.5 [−8.0]	−1.0 [−2.0]	−1.5 [−8.0]	−17.5 [−5.5]	−2.0 [−2.5]	−6.0 [−14.5]
B4		3′-CAC **B**AT ACG											
B2	+1	5′-GTG A**B**A TGC		+16.0 [+2.0]	−5.5 [−8.5]	+2.5 [**−27.0**]	−1.5 [**−40.0**]	+1.0 [**−31.0**]	−5.5 [**−18.0**]	−2.0 [**−29.0**]	−10.0 [**−17.0**]	+0.5 [**−12.0**]	−2.0 [**−26.0**]
B5		3′-CAC TA**B** ACG											
B2	−1	5′-GTG A**B**A TGC		+7.0 [+2.5]	−5.5 [−5.5]	+15.5 [−5.0]	+26.0 [−3.5]	+26.5 [+1.0]	+9.5 [+3.0]	+13.0 [−2.5]	−8.5 [−5.5]	+5.5 [−2.5]	+10.5 [−5.5]
B4		3′-CAC **B**AT ACG											
B3	−1	5′-GTG ATA **B**GC		+8.5 [−2.5]	−2.5 [−4.0]	+18.0 [−8.0]	+25.0 [−8.5]	+29.5 [+1.5]	–	–	–	–	+14.0 [−5.5]
B5		3′-CAC TA**B** ACG											
B3	−3	5′-GTG ATA **B**GC		+8.0 [+1.5]	−2.5 [−1.0]	+18.0 [+1.0]	+28.5 [+4.0]	+22.0 [+0.5]	–	–	–	–	+10.5 [−1.0]
B4		3′-CAC **B**AT ACG											

[a] ΔT_m = change in T_m values relative to unmodified reference duplex **D1**:**D2** ($T_m \equiv 29.5$ °C); see Table 1 for the experimental conditions; example of DA calculation: DA (**W1**:**W5**) = ΔT_m (**W1**:**W5**) − [ΔT_m (**W1**:**D2**) + ΔT_m (**D1**:**W5**)] = 25.0 °C - [7.0 °C + 15.5 °C] = +2.5 °C. [b] Previously reported in ref 29.

unmodified DNA duplexes because of additive contributions from the two monomers and (ii) not activated for dsDNA recognition (i.e., $\Delta T_m \gg 0$ °C and DA ≈ 0 °C; Table 3). While rather stable, double-stranded probes with −1 interstrand zippers of **W** monomers display less-than-additive increases in thermostability and are weakly activated for dsDNA recognition (i.e., $\Delta T_m \gg 0$ °C and DA < 0 °C; Table 3). Duplexes with +2 and in particular +1 zippers are far less stable and more strongly activated (i.e., $\Delta T_m \approx 0$ °C and DA ≪ 0 °C; Table 3). As previously mentioned, +1 zippers of **W** monomers are the structural elements that were used to realize Invader-mediated recognition of isosequential dsDNA targets in our original studies.[29,31]

In contrast, control duplexes with two conventional 2′-oxy-α-L-LNA thymine monomers are highly thermostable, regardless of the relative monomer arrangement, because of additive contributions from the two monomers (i.e., $\Delta T_m \gg 0$ °C and DA ≈ 0 °C; data for **O** monomers in Table 3). Duplexes with two 2′-amino-α-L-LNA thymine (**N**) monomers in +4/+2/−3 arrangements are not thermally activated for dsDNA recognition, while duplexes with +1/−1 zippers are mildly activated (DA between −8.5 and −4.0 °C; Table 3). We speculate that the latter is a result of electrostatic repulsion between two proximal and partially protonated 2′-amino-α-L-LNA monomers. These control experiments demonstrate that the pyrenes of the two **W** monomers play a key role in activating the +1 zipper probe **W2**:**W5**, whereas the presence of two proximal α-L-LNA skeletons is less important. This suggested to us that non-LNA-based monomers could be used to activate double-stranded probes for dsDNA recognition via the approach depicted in Figure 1.

The hybridization characteristics of duplexes with interstrand arrangements of two 2′-*N*-(pyren-1-yl)carbonyl-2′-amino-α-L-LNA thymine (**X**) monomers resemble those of the corresponding **W** series (Table 3), namely, roughly additive contributions in thermostability with +4 and −3 zippers, mildly antagonistic effects with −1 zippers, and strong activation with +2 and +1 zippers. Interestingly, +1 zipper duplex **X2**:**X5** is more strongly activated than **W2**:**W5** ($DA_{X2:X5}$ = −40.0 °C; Table 3).

Duplexes with interstrand zippers of monomers **Y** or **Z**, which feature longer linkers between the pyrene and sugar moieties, are progressively less activated than the **X** series (i.e., less negative DA values; Table 3). This likely reflects less efficient intercalation of the pyrenes. Nonetheless, duplexes with +1 zippers are still strongly activated for dsDNA recognition.

Duplexes with interstrand arrangements of two 2′-*N*-methyl-2′-*N*-(pyren-1-yl)methyl-2′-aminodeoxyuridine (**Q**) or 2′-*O*-(pyren-1-yl)methyluridine (**P**) monomers display similar characteristics as the **W** series (Table 3), including DA values for +1 zipper duplexes **Q2**:**Q5** and **P2**:**P5** similar to those for **W2**:**W5**, which supports our hypothesis that **Q** and **P** are functional mimics of the original Invader LNA monomer.

Duplexes with interstrand zippers of N2′-acylated 2′-*N*-methyl-2′-aminodeoxyuridine monomers **S** or **V** generally display low thermostability and are moderately activated regardless of the interstrand monomer arrangement (DA < 0 °C; Table 3). **S2**:**S5** and **V2**:**V5** are the least activated examples of double-stranded probes with +1 zippers of pyrene-functionalized monomers studied herein.

To sum up the thermal denaturation characteristics of DNA duplexes with different interstrand zipper arrangements of pyrene-functionalized monomers, +1 interstrand zippers consistently result in the most pronounced thermal activation of double-stranded probes (i.e., compare the DA values of **B2**:**B5** in Table 3 with those of other monomer arrangements). The level of activation is monomer-dependent and decreases in the following order: **X** > **Y** ≥ **Q** ≥ **W** ≥ **P** > **Z** ≥ **S** > **V** (DA values for **B2**:**B5** in Table 3).

Similar trends were observed for duplexes with interstrand zipper arrangements of pyrene-functionalized adenine monomers **K**, **L**, **M**, and **R** (Table 4). Thus, duplexes with +1 interstrand zippers display low thermostability and strongly negative DA values (see data for **B6**:**B8** and **B7**:**B9** in Table 4), while duplexes with +3 or −1 zippers generally are highly

dx.doi.org/10.1021/jo4015936 | J. Org. Chem. 2013, 78, 9560−9570

Table 4. ΔT_m and DA Values for DNA Duplexes with Interstrand Zipper Arrangements of Pyrene-Functionalized Adenine Monomers[a]

			ΔT_m/°C [DA/°C]			
ON	zipper	duplex	for **B** =	**K**	**L**	**M**	**R**
B6	+3	5′-GTG **B**TA TGC		+12.0 [+1.5]	+13.0 [−10.0]	+16.0 [+4.0]	+10.0 [−1.0]
B9		3′-CAC TAT **B**CG					
B6	+1	5′-GTG **B**TA TGC		−7.0 [**−18.5**]	−8.0 [**−30.5**]	−7.5 [**−21.0**]	−7.5 [**−20.5**]
B8		3′-CAC T**B**T ACG					
B7	+1	5′-GTG AT**B** TGC		−5.0 [**−17.5**]	−7.0 [**−33.0**]	−8.0 [**−21.5**]	−7.0 [**−22.0**]
B9		3′-CAC TAT **B**CG					
B7	−1	5′-GTG AT**B** TGC		+14.0 [+0.5]	+23.5 [−2.0]	+22.0 [+7.0]	+15.0 [−2.0]
B8		3′-CAC T**B**T ACG					

[a] ΔT_m = change in T_m value relative to the unmodified reference duplex **D1**:**D2** (T_m = 29.5 °C); see Table 1 for the experimental conditions.

thermostable as a result of additive contributions from the two monomers. Moreover, the relationships between the DA values and the linker chemistry and length resemble those observed for the corresponding thymine analogues (trend in DA values for +1 zippers: **L** > **M** ≥ **K** vs **X** > **Y** ≥ **W**; Tables 3 and 4). Furthermore, duplexes with +1 zippers of **R** monomers display similar DA values as the corresponding duplexes composed of the synthetically more elaborate **K** monomers.

Importantly, the results demonstrate that Invaders can be constructed using pyrimidine as well as purine building blocks, which is necessary if sequence-unrestricted recognition of dsDNA is to be realized.

The thermostability of duplexes with "mixed" interstrand arrangements of *N*2′-pyrene-functionalized 2′-amino-α-L-LNA adenine monomers **K** and **L** (i.e., one strand modified with monomer **K** and the other strand modified with monomer **L**) was also evaluated (Table S2 in the Supporting Information). Briefly described, the observed DA values are intermediate between those observed for the corresponding duplexes with zippers composed of only one monomer. For example, duplexes with "mixed" +1 zippers display DA values between −19.5 and −23.0 °C. Thus, Invaders can be designed with +1 zippers that are composed of different monomers, although there is no clear advantage to this approach.

The thermostability of duplexes in which one strand is modified with an *N*2′-pyrene-functionalized 2′-amino-α-L-LNA thymine monomer (**W** or **X**) and the other strand is modified with a corresponding adenine monomer (**K** or **L**) was also evaluated (Tables S3−S6 in the Supporting Information). The results can be briefly described as follows: (i) duplexes with −2 interstrand zippers are highly thermostable because of additive contributions from the two monomers (i.e., $\Delta T_m \gg 0$ °C and DA ≈ 0 °C); (ii) duplexes with +2 zippers are thermally activated but rather thermostable ($\Delta T_m \gg 0$ °C; DA between −19.0 and −10.5 °C); and (iii) duplexes with 0 zippers are generally more strongly activated than duplexes with +2 zippers (DA between −22.0 and −10.0 °C) and vary from weakly to highly thermostable (ΔT_m between −4.5 and +12.5 °C). Very similar trends were observed for duplexes in which one strand is modified with a 2′-*O*-(pyren-1-yl)methyluridine monomer **P** and the other strand is modified with a corresponding adenine monomer **R** (Table S7 in the Supporting Information) .

To sum up, duplexes with +1 zippers of pyrene-functionalized monomers are the most strongly activated constructs for dsDNA recognition via the Invader approach (i.e., lowest DA values). While Invaders based on 2′-*N*-(pyren-1-yl)carbonyl-2′-amino-α-L-LNA monomers are most strongly activated, Invaders modified with the synthetically simpler 2′-*N*-methyl-2′-*N*-(pyren-1-yl)methyl-2′-amino-DNA and 2′-*O*-(pyren-1-yl)methyl-RNA monomers also have prominent dsDNA recognition potential.

Steady-State Fluorescence Emission Spectra of Duplexes with Interstrand Arrangements of Pyrene-Functionalized Monomers. As a first step toward rationalizing the observed thermostability trends, steady-state fluorescence emission spectra of duplexes with different interstrand arrangements of pyrene-functionalized monomers were recorded at 5 °C using an excitation wavelength (λ_{ex}) of 350 nm (Figure 3). Interestingly, duplexes with +1 interstrand monomer arrangements have distinctly different emission profiles than duplexes with other zippers. For example, **W2**:**W5** and **Y2**:**Y5** display structured pyrene monomer peaks at emission wavelengths (λ_{em}) of ∼380 and ∼400 nm, respectively, along with a dominant excimer emission at $\lambda_{em} \approx 490$ nm, which implies a coplanar arrangement of pyrene moieties with an interplanar separation of ∼3.4 Å.[41] Duplexes with +1 zippers of monomers **Q**, **V**, **P**, **M**, or **R** display weak pyrene−pyrene excimer emission in addition to monomer emission (Figure 3). With the exception of **P1**:**P4**, duplexes with other interstrand arrangements of pyrene-functionalized monomers display no or minimal excimer emission, indicating that interactions between pyrene moieties are negligible. We speculate that the intense excimer emission of +2 zipper duplex **P1**:**P4** is a result of pyrene−pyrene stacking interactions in the grooves, in a similar manner as observed for DNA duplexes with +2 zipper arrangements of pyrene-functionalized *ara*-uridine monomers.[42−44] Interestingly, +1 zipper duplexes **X2**:**X5** and **S2**:**S5**, which are composed of (pyren-1-yl)carbonyl-functionalized monomers, do not display excimer emission but instead feature monomer emission that is considerably more intense than in duplexes with other interstrand arrangements.

There are many reports of duplexes with interstrand zipper arrangements of pyrene-functionalized monomers in which excimer-emitting pyrene dimers are formed in the grooves[42−52] or duplex core.[26,29,31,53−55] In view of the fact that intercalation of the pyrene moieties is expected to be the primary binding mode for the monomers reported herein,[32,34,36,40] stacking of the pyrenes inside the duplex core appears to be the most plausible binding mode for double-stranded probes with +1 interstrand monomer arrangements.

dx.doi.org/10.1021/jo4015936 | J. Org. Chem. 2013, 78, 9560−9570

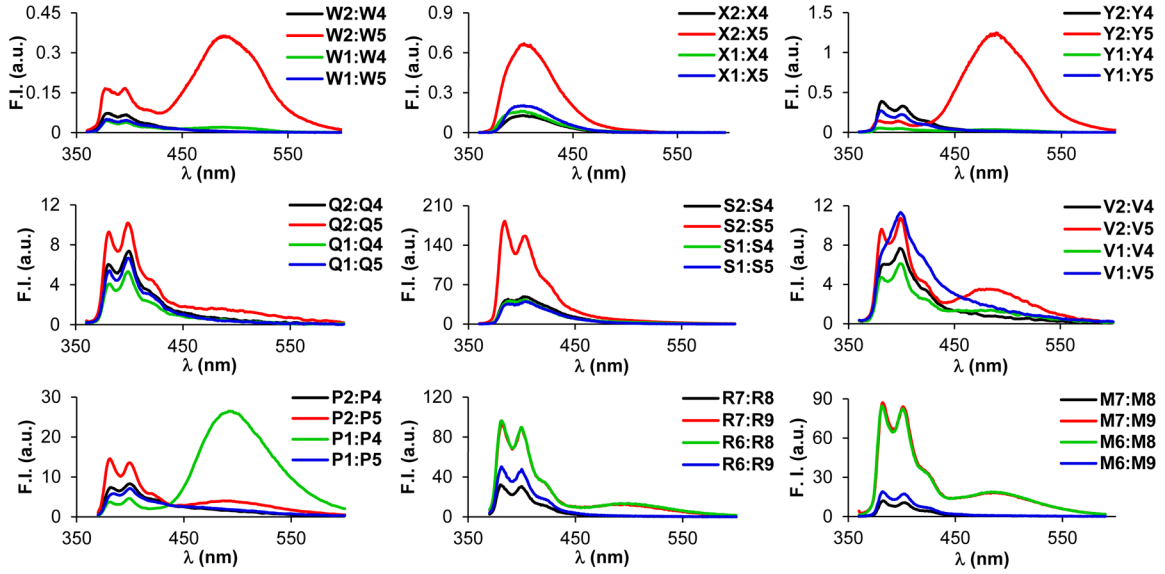

Figure 3. Steady-state fluorescence emission spectra of duplexes with different interstrand arrangements of selected pyrene-functionalized monomers. The spectra were recorded in thermal denaturation buffer at T = 5 °C with each strand at 1.0 μM and λ_{ex} = 350 nm. It should be noted that different Y-axis scales are used.

Molecular Modeling Studies of W2:W5. To gain additional insight into the structural factors that govern the thermal activation of duplexes with +1 interstrand zippers of pyrene-functionalized nucleotides, we performed a molecular modeling study on **W2:W5**. In brief, the duplex was initially built with a standard B-type helix geometry and subjected to a Monte Carlo search using the AMBER94 force field[56] with the improved parambsc0 parameter set[57] and the GB/SA solvation model[58] as implemented in MacroModel version 9.8.[59] Representative examples of the resulting structures were subsequently used as seed structures for stochastic dynamics simulations (5 ns; 300 K) during which structures were collected at regular intervals and energy-minimized. The lowest-energy structure obtained via this protocol displays intercalation of one pyrene moiety, while the other is projected into the major groove (Figure S1 in the Supporting Information). Since this structure did not account for the observed excimer emission of **W2:W5**, we examined structures of higher energy. In one ensemble of structures, the pyrene moieties of both **W** monomers intercalate into the duplex core and engage in mutual stacking interactions (Figure 4). Specific 3′-directed intercalation of the pyrene moieties results in molecular crowding, duplex extension (*rise* = 10.6 Å), and unwinding (*twist* = 23°, 20°, and 24° for A_4T_{15}–$\mathbf{W}_5A_{14}$, $\mathbf{W}_5A_{14}$–$A_6\mathbf{W}_{13}$, and $A_6\mathbf{W}_{13}$–T_7A_{12}; numbering: 5′-$G_1T_2G_3A_4\mathbf{W}_5A_6T_7G_8C_9$ and 3′-$C_{18}A_{17}C_{16}T_{15}A_{14}\mathbf{W}_{13}A_{12}C_{11}G_{10}$) relative to the corresponding unmodified DNA duplex (*rise* = 3.3 Å; *twist* = 31°, 30° and 31°; results not shown). Moreover, the pyrene–pyrene interaction perturbs the stacking interaction between the pyrene and thymine moieties of a **W** monomer (Figure 4, upper right). We previously observed these interactions in modeling of structures of singly modified DNA duplexes and proposed them as key factors for the affinity-enhancing properties of **W** monomers.[32] Moreover, the pyrene moieties of **W2:W5** engage in stacking interactions with the 3′-flanking nucleobase on "their own" strand but interact very little with the thymine of the **W** monomer in the +1 position on the opposite strand. As a result, the flanking base pairs are strongly bent (*buckle* = 20° and −35° for $\mathbf{W}_5A_{14}$ and $A_6\mathbf{W}_{13}$, respectively) relative to the corresponding unmodified DNA duplex (*buckle* = 6° and −4° for T_5A_{14} and A_6T_{13}, respectively).

The structural model of **W2:W5** shown in Figure 4 accounts for the observed excimer emission and thermal activation. The duplex perturbation in the vicinity of the +1 zipper arrangement of the **W** monomers likely reflects a violation of the "nearest-neighbor exclusion principle", which states that free intercalators at most bind to every second base pair of a DNA duplex because of limits in the local expandability of duplexes.[60] A +1 interstrand arrangement of **W** monomers results in a localized region with one intercalator per base pair (Figure 4). Similar structural consequences have been observed in NMR structures of DNA duplexes with adjacent incorporations of pyrene-modified non-nucleotide monomers.[33]

Given the similarities in hybridization and fluorescence emission characteristics, we speculate that duplexes with +1 zipper arrangements of the other pyrene-functionalized monomers studied herein adopt similar duplex structures.

NMR Studies of a DNA Duplex with a +1 Interstrand Zipper of W Monomers. Next, we performed NMR studies on a 13-mer DNA duplex with a single +1 interstrand arrangement of **W** monomers to substantiate the structural hypothesis established from molecular modeling (**W13a:W13b**: T_m = 41.0 °C, ΔT_m = +3.5 °C, DA = −17.5 °C; Figure 5).[31] The 800 MHz ^{1}H NMR spectrum of **W13a:W13b** in 95% H_2O (T = 25 °C) exhibits several imino resonances between 12.7 and 13.5 ppm (Figure 5, top), which implies the formation of Watson–Crick base pairs. However, the low number of observable signals does not fully satisfy the suggested base-pairing pattern of **W13a:W13b**. The 2D NOESY spectrum of **W13a:W13b** confirms that complementary duplexes are formed in solution (Figure S2 in the Supporting Information). However, the NMR resonances assigned to nucleotides near monomer **W** get progressively broader, and the signals of protons that are spatially close to the pyrene moieties are not observed at all (Figure 5, bottom). Thus, no aromatic or sugar resonances could be observed for residues W5–T7 and W8–T10 in the **W13a** and **W13b** strands, respectively; also, the T3 and T9 imino resonances of the **W13a** strand and the T6 imino

dx.doi.org/10.1021/jo4015936 | J. Org. Chem. 2013, 78, 9560–9570

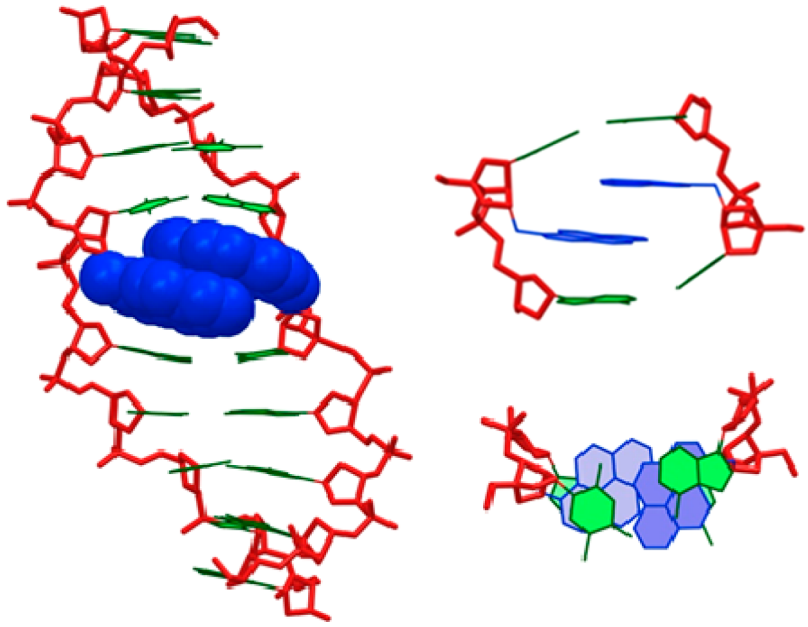

Figure 4. Energy-minimized structure of **W2:W5**. Left: side view of the duplex. Upper right: alternative representation of the central duplex region. Bottom right: top view of the central duplex region. Color code: sugar phosphate backbone (red); pyren-1-ylmethyl moieties of **W** monomers (blue); nucleobases (green). H atoms, Na^+ ions, and bond orders have been omitted for clarity.

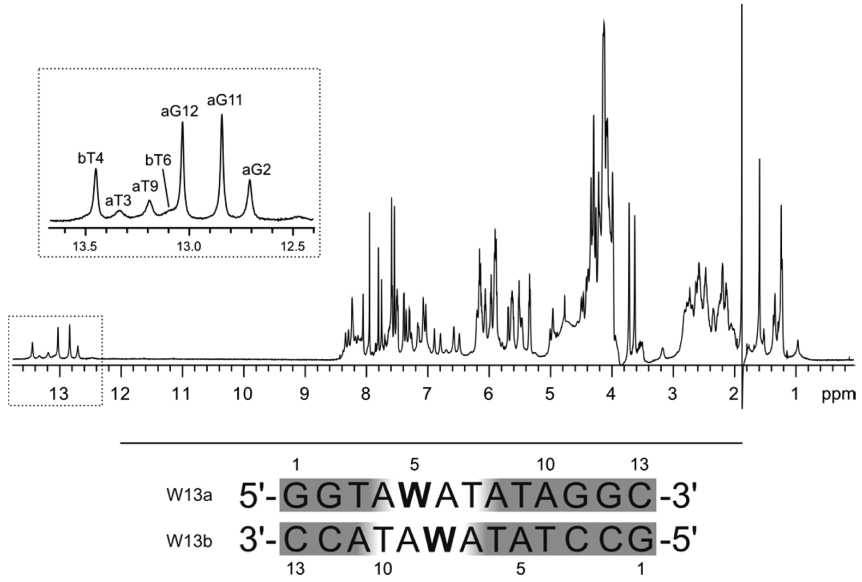

Figure 5. Top: ^{1}H NMR spectrum of **W13a:W13b** recorded in 95% H_2O at 25 °C. The assignment of imino resonances is shown in the inset, with the first letter of each assignment indicating either the **a** or **b** strand of the duplex. Bottom: sequences of **W13a:W13b** and numbering of nucleotides; shaded nucleotides denote regions with observable NMR signals.

resonance of the **W13b** strand exhibit considerable broadening (inset of Figure 5, top). Several magnetic fields, fast and slow annealing procedures, and temperatures ranging from 0 to 35 °C were explored in unsuccessful attempts to observe the missing resonances. Temperature variation resulted in only minor changes in the ^{1}H chemical shifts and peak intensities.

Hence, the results substantiate that +1 interstrand zippers of **W** monomers induce significant local perturbation of probe duplexes, which explains their relatively low thermostabilities.

Invader-Mediated Recognition of DNA Hairpins. Next, we examined the dsDNA-targeting characteristics of double-stranded probes with interstrand arrangements of pyrene-functionalized monomers. Assuming that efficient recognition of dsDNA targets requires probes that are thermally activated and display low thermostability (i.e., DA $\ll$ 0 °C and $\Delta T_m \leq 0$ °C), we decided to focus our efforts on probes with +1 interstrand monomer arrangements.

In our original studies, we demonstrated using fluorescence-based assays that **W**-modified Invaders efficiently recognize 9- and 13-mer dsDNA targets under conditions designed to minimize strand exchange between probes and targets ($[Na^+]$ = 110−710 mM; $T_{experimental} < T_m$).[29,31] To evaluate Invaders in a more challenging assay, we recently introduced an assay based on electrophoretic mobility shift,[37] a version of which was used herein. Thus, a digoxigenin (DIG)-labeled DNA hairpin (DH) comprising a 9-mer double-stranded stem linked together via a

dx.doi.org/10.1021/jo4015936 | J. Org. Chem. 2013, 78, 9560−9570

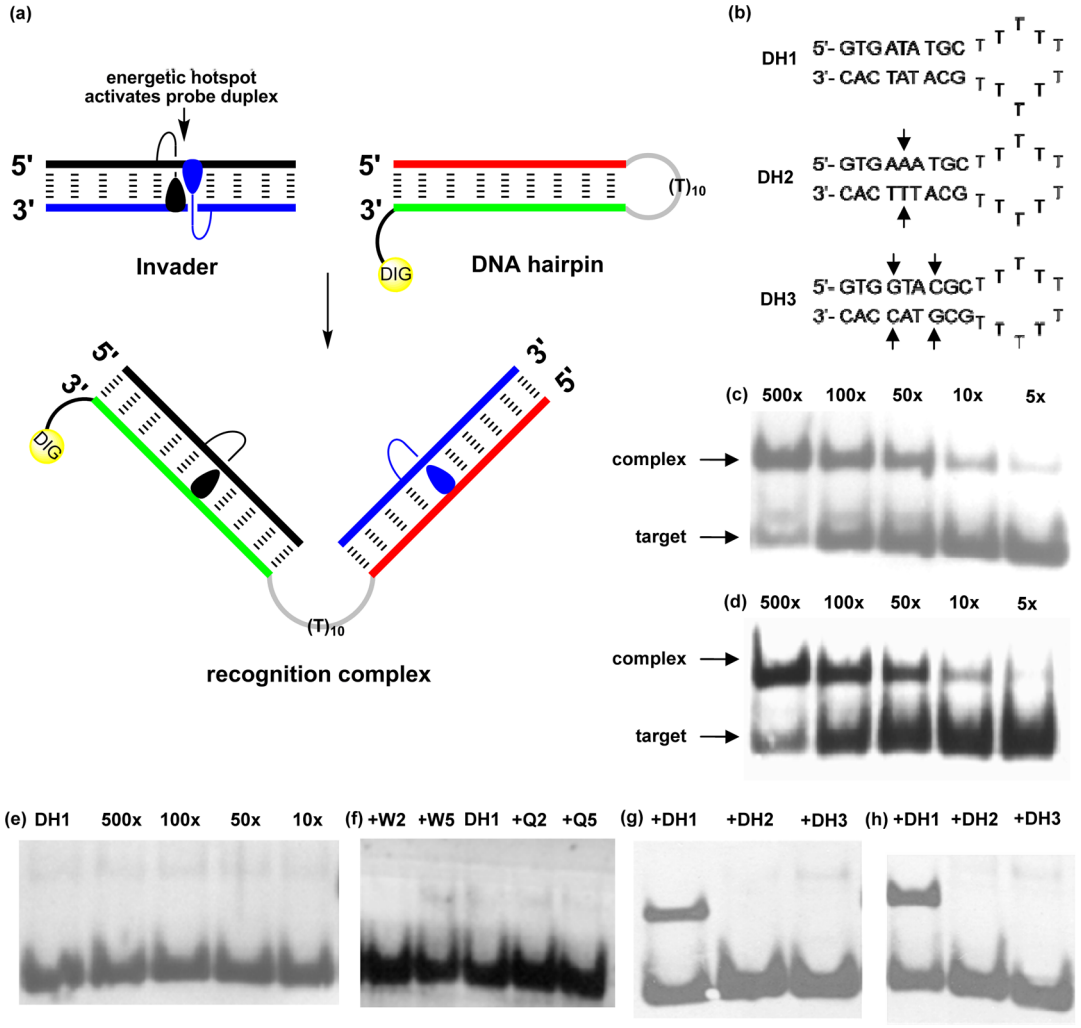

Figure 6. Recognition of structured dsDNA targets by Invader probes using electrophoretic mobility shift assays. (a) Illustration of the recognition process. (b) Structures of DNA hairpins with isosequential (**DH1**) or nonisosequential (**DH2** and **DH3**) stem regions (arrows denote points of deviation). (c–e) Incubation of **DH1** with varying excesses of **W2**:**W5**, **Q2**:**Q5**, or **D1**:**D2**, respectively. (f) Incubation of **DH1** with a 100-fold excess of single-stranded **W2**, **W5**, **Q2** or **Q5**; (g, h) Incubation of **DH1**–**DH3** with a 100-fold excess of **W2**:**W5** or **Q2**:**Q5**, respectively. Probe–target incubation: 3 h at 20 °C, 15% nondenaturing PAGE. DIG = digoxigenin.

T_{10} loop served as the model dsDNA target (Figure 6a,b). The unimolecular nature of the DNA hairpin confers significant stability to the stem region [T_m(**DH1**) = 56.0 °C vs T_m(**D1**:**D2**) = 29.5 °C]. Invader-mediated binding to the DNA hairpin is expected to form recognition complexes with lower electrophoretic mobility on nondenaturing PAGE gels than unreacted DNA hairpins (Figure 6a).

Indeed, incubation of Invader LNA **W2**:**W5** with DNA hairpin **DH1** (~3 h, rt) resulted in dose-dependent formation of slower-moving recognition complexes (Figure 6c). While only trace amounts of complex were observed when a 5-fold molar excess of **W2**:**W5** was used, ~50% mixed-sequence recognition was realized with a 100-fold excess (Figure 6c, Table 5, and Figure S3 in the Supporting Information). Interestingly, moderately activated Invaders displayed poor recognition efficiency (i.e., **S2**:**S5**, **V2**:**V5**, **K6**:**K8**, and **M6**:**M8**: DA ≥ −21 °C, < 20% recognition at 100-fold excess; Table 5), whereas strongly activated Invaders recognized DNA hairpins with high and remarkably similar efficiency (i.e., DA < −21 °C, 40–50% recognition at 100-fold excess; Figure 6c,d, Table 5, and Figures S3 and S4 in the Supporting Information). The latter group includes Invaders modified with *N*2′-pyrene-functionalized 2′-amino-α-L-LNA **X** or **Y** monomers, synthetically less elaborate **P** or **Q** monomers, and adenine monomer **R**. Importantly, none of the following control experiments produced appreciable amounts of recognition complexes:[61] (a) incubation of up to a 500-fold excess of unmodified DNA duplex **D1**:**D2** with DNA hairpin **DH1** (Figure 6e); (b) incubation of a 100-fold excess of single-stranded **W2**/**W5**/**Q2**/**Q5**/**P2**/**P5**/**R6**/**R8** with DNA hairpin **DH1** (Figure 6f and Figure S5 in the Supporting Information); and (c) incubation of a 100-fold excess of selected Invader **W2**:**W5**, **Q2**:**Q5**, **X2**:**X5**, **Y2**:**Y5**, or **K6**:**K8** with DNA hairpin **DH2** or **DH3** featuring fully base-paired but nonisosequential stem regions [one or two base pair deviations relative to Invaders; T_m(**DH2**) = 57.0 °C, T_m(**DH3**) = 64.5 °C] (Figure 6g,h and Figure S6 in the Supporting Information).

Thus, the results demonstrate that Invaders composed of a variety of pyrene-functionalized nucleotides can recognize the double-stranded stems of DNA hairpins. The control experiments show that (i) the energetic hotspots play a critical role in activating Invaders for mixed-sequence dsDNA recognition, (ii) both strands of an Invader probe are required for the recognition to take place, and (iii) Invader-mediated dsDNA recognition proceeds with excellent binding specificity. In view

dx.doi.org/10.1021/jo4015936 | J. Org. Chem. 2013, 78, 9560–9570

Table 5. Efficiency of Hairpin Invasion of Various Invaders at 100-Fold Probe Excess[a]

ON	Invader	% recognition
W2	5′-GTG A**W**A TGC	48 ± 11
W5	3′-CAC TA**W** ACG	
X2	5′-GTG A**X**A TGC	41 ± 12
X5	3′-CAC TA**X** ACG	
Y2	5′-GTG A**Y**A TGC	38 ± 2
Y5	3′-CAC TA**Y** ACG	
Q2	5′-GTG A**Q**A TGC	45 ± 14
Q5	3′-CAC TA**Q** ACG	
S2	5′-GTG A**S**A TGC	<5
S5	3′-CAC TA**S** ACG	
V2	5′-GTG A**V**A TGC	<5
V5	3′-CAC TA**V** ACG	
P2	5′-GTG A**P**A TGC	47 ± 3
P5	3′-CAC TA**P** ACG	
K6	5′-GTG **K**TA TGC	17 ± 3
K8	3′-CAC T**K**T ACG	
M6	5′-GTG **M**TA TGC	<5
M8	3′-CAC T**M**T ACG	
R6	5′-GTG **R**TA TGC	41 ± 4
R8	3′-CAC T**R**T ACG	

[a]Averages of three independent measurements; " ± " denotes standard deviation. For the experimental conditions, see Figure 6.

of the important roles that DNA hairpins play in the regulation of gene expression,[62,63] hairpin-targeting Invaders can be envisioned as molecular tools for the study of these processes. While the DNA hairpins studied here represent a lower level of complexity than long DNA duplexes and dsDNA in tightly packaged chromatin, we are very encouraged to note that second-generation Invaders already have been shown to recognize mixed-sequence chromosomal DNA regions in the context of nondenaturing FISH experiments.[37]

■ CONCLUSION

In the present study, we have demonstrated that incorporation of +1 interstrand zippers of intercalator-functionalized nucleotides is a general strategy for activation of double-stranded probes for mixed-sequence dsDNA recognition via a dual duplex invasion mechanism that relies on differences in thermostability between probes and probe−target duplexes. Our structural studies strongly suggest that Invaders are destabilized by the duplex distortion that ensues when two intercalating pyrene moieties positioned in a +1 zipper compete for the same region in the duplex core. Importantly, we have demonstrated that the key features of these "energetic hotspots" can be emulated using 2′-*O*-(pyren-1-yl)methyl-RNA or 2′-*N*-methyl-2′-*N*-(pyren-1-yl)methyl-2′-amino-DNA monomers. Thus, Invaders modified with these building blocks recognize DNA hairpins with efficiencies similar to those of Invaders based on the original 2′-*N*-(pyren-1-yl)methyl-2′-amino-α-L-LNA monomers. Identification of synthetically simple yet efficient monomers represents an important practical advance that will facilitate systematic structure−property studies and accelerate the use of Invaders for applications in molecular biology and nucleic acid diagnostics. In fact, second-generation Invaders have already been demonstrated to recognize mixed-sequence chromosomal DNA regions in the context of nondenaturing FISH experiments.[37] Studies aimed at further refinement of the Invader approach into a general strategy for mixed-sequence recognition of dsDNA are ongoing and will be reported shortly.

■ EXPERIMENTAL SECTION

Synthesis of Functionalized Oliogonucleotides. The majority of the ONs used in the present study were prepared and characterized with respect to identity (MALDI-MS) and purity (>80%, ion-pair RP-HPLC) in conjunction with previous studies.[32,34,38,40] **P3** was synthesized in a similar fashion as other **P**-modified ONs.[34] Novel ONs **R6**−**R9**, which are modified with the 2′-*O*-(pyren-1-yl)-methyladenosine monomer **R**,[64] were synthesized via machine-assisted solid-phase DNA synthesis (0.2 μmol scale, 500 Å succinyl-linked LCAA−CPG support) using extended coupling times (4,5-dicyanoimidazole as the activator, 15 min, ∼98% coupling yield) during incorporation of the corresponding A^{Bz}-protected phosphoramidite of monomer **R**. The ONs were worked up, purified by RP-HPLC, and characterized with respect to identity (MALDI-MS) and purity (>80%, ion-pair RP-HPLC) following our standard protocols.[34]

Thermal Denaturation Studies. The concentrations of all ONs were estimated using the following extinction coefficients (in L $mmol^{-1}$ cm^{-1}) at 260 nm: dA (15.20), dC (7.05), dG (12.01), T (8.40); pyrene (22.40). ONs (1.0 μM each strand) were thoroughly mixed in T_m buffer (see below), denatured by heating, and subsequently cooled to the starting temperature of the experiment. Thermal denaturation curves (A_{260} vs T) were recorded using a UV/vis spectrometer equipped with a Peltier temperature programmer. The temperature was varied from at least 15 °C below to 15 °C above the thermal denaturation temperature using a ramp of 0.5 °C min^{-1}. Quartz optical cells with a path length of 10 mm were used. A medium-salt T_m buffer was used (100 mM NaCl, 0.1 mM EDTA, pH 7.0 adjusted with 10 mM NaH_2PO_4 and 5 mM Na_2HPO_4). Thermal denaturation temperatures were determined from the first derivatives of the thermal denaturation curves using the software provided with the UV/vis spectrometer. The reported thermal denaturation temperatures were determined as averages of two separate experiments within ±1.0 °C.

Molecular Modeling Protocol. An unmodified DNA duplex was built in a standard B-type geometry and subsequently modified within MacroModel version 9.8[59] to provide a starting structure of **W2**:**W5**. The charge of the phosphodiester backbone was neutralized with sodium ions, which were placed 3.0 Å from the two nonbridging oxygen atoms. The starting structure was then subjected to a Monte Carlo conformational search. The conformational space was sampled by varying the N2′−CH_2 and CH_2−$C1_{Py}$ torsion angles of monomers **W**; 55 998 structures were generated and minimized using the AMBER94 force field[56] with the improved parambsc0 parameter set,[57] the GB/SA solvation model,[58] and the Polak−Ribiere conjugate gradient method (convergence criteria 0.1 kJ mol^{-1} $Å^{-1}$) as implemented in MacroModel version 9.8.[59] The original AMBER94 parameters were used for monomer **W** and the 3′-neighboring nucleotide. Nonbonded interactions were treated with extended cutoffs (8.0 Å for van der Waals and 20.0 Å for electrostatics). All atoms were allowed to move freely during minimization except for the following distance restraints: (a) sodium ions were restrained to 3.0 Å from the two nonbridging oxygen atoms of the corresponding phosphodiester groups by a force constant of 100 kJ mol^{-1} $Å^{-2}$ and (b) the hydrogen-bonding distances between the thymine moiety of monomer **W** and its Watson−Crick partner [(T)N3−H···N1(A), 1.85 Å; (T)O4···H−N6(A), 1.81 Å] and of the outermost base pairs [(C)O2···H−N2(G),

dx.doi.org/10.1021/jo4015936 | J. Org. Chem. 2013, 78, 9560−9570

1.98 Å; (C)N3···H–N1(G), 1.94 Å; (C)N4–H···O6(G), distance 1.89 Å] were restrained by a force constant of 100 kJ mol^{-1} $Å^{-2}$.

Twelve representative low-energy structures were subsequently submitted to 5 ns of stochastic dynamics (simulation temperature 300 K; time step 2.2 fs; SHAKE all bonds to hydrogen; same distance restraints as during the Monte Carlo search) during which 500 structures were sampled at regular time intervals to allow conformational analysis and energy minimization (convergence criteria 0.05 kJ mol^{-1} $Å^{-1}$).

NMR Spectroscopy. Equimolar amounts of **W13a** and **W13b** were dissolved in 95% H_2O, 5% ^2H_2O with the addition of NaCl (50 mM) and sodium phosphate buffer (pH 6.7). All NMR spectra were acquired on 800 and 600 MHz NMR spectrometers equipped with cold and room-temperature triple probes, respectively. 2D NOESY spectra were used for the sequential assignment and were acquired with τ_m values of 80, 150, and 250 ms. 2D TOCSY spectra were used for the identification of pyridine H5 resonances and were acquired with τ_m = 80 ms (data not shown). All experiments were performed on a natural-abundance sample at temperatures ranging from 0 to 35 °C. NMR spectra were processed and analyzed using VNMRJ (Varian Inc.) and Sparky (UCSF) software.

Invader-Mediated Recognition of DNA Hairpins: Electrophoretic Mobility Shift Assays. These assay, which were conducted in lieu of footprinting experiments to avoid the use of ^{32}P-labeled targets, were performed in a similar manner as previously described.[37] Thus, ∼100 pmol samples of unmodified **DH1–DH3** were 3′-DIG-labeled using the second-generation DIG gel shift kit (Roche Applied Bioscience) as recommended. Equal volumes of 100 nM solutions of DIG-labeled dsDNA targets and probe solutions (concentrations: 0.5, 1, 5, 10, and 50 μM) in 1× HEPES buffer (50 mM HEPES, 100 mM NaCl, 5 mM $MgCl_2$, pH 7.2, 10% sucrose, 1 mg/mL spermine tetrahydrochloride) were mixed and incubated for 3 h at room temperature before being loaded on a 15% nondenaturing polyacrylamide gel. After 2–3 h of electrophoresis at 100 V in a cold room (∼4 °C) using TBM (89 mM Tris, 89 mM boric acid, 10 mM $MgCl_2$) as a running buffer, the nucleic acid complexes were transferred to a positively charged nylon membrane by electroblotting and processed as recommend by the manufacturer of the DIG gel shift kit. The chemiluminescence was captured on an X-ray film, and the bands were quantified using Quantity One software.

■ ASSOCIATED CONTENT

Supporting Information

MS data for **R**-modified ONs; thermal denaturation properties of double-stranded probes with "mixed" zippers; lowest-energy structure of **W2:W5**; NOESY spectrum of **W13a:W13b**; dose–response curves; and additional gel electropherograms. This material is available free of charge via the Internet at http://pubs.acs.org.

■ AUTHOR INFORMATION

Corresponding Author

*hrdlicka@uidaho.edu

Notes

The authors declare the following competing financial interest(s): P.J.H. is the inventor of intellectual property involving the Invader technology.

■ ACKNOWLEDGMENTS

This study was supported by Award R01 GM088697 from the National Institute of General Medical Sciences, National Institutes of Health; Award IF13-001 from the Higher Education Research Council, Idaho State Board of Education; Idaho NSF EPSCoR; the BANTech Center at the University of Idaho; the Slovenian Research Agency (ARRS, P1-0242 and J1-4020); the Danish National Research Foundation; and the Danish Agency for Science Technology and Innovation.

■ REFERENCES

(1) Rogers, F. A.; Lloyd, J. A.; Glazer, P. M. *Curr. Med. Chem.: Anti-Cancer Agents* **2005**, *5*, 319–326.
(2) Ghosh, I.; Stains, C. I.; Ooi, A. T.; Segal, D. J. *Mol. BioSyst.* **2006**, *2*, 551–560.
(3) Nielsen, P. E. *ChemBioChem* **2010**, *11*, 2073–2076.
(4) Mukherjee, A.; Vasquez, K. M. *Biochimie* **2011**, *93*, 1197–1208.
(5) Aiba, Y.; Sumaoka, J.; Komiyama, M. *Chem. Soc. Rev.* **2011**, *40*, 5657–5668.
(6) Vaijayanthi, T.; Bando, T.; Pandian, G. N.; Sugiyama, H. *ChemBioChem* **2012**, *13*, 2170–2185.
(7) Simon, P.; Cannata, F.; Concordet, J.-P.; Giovannangeli, C. *Biochimie* **2008**, *90*, 1109–1116.
(8) Duca, M.; Vekhoff, P.; Oussedik, K.; Halby, L.; Arimondo, P. B. *Nucleic Acids Res.* **2008**, *36*, 5123–5138.
(9) Kaihatsu, K.; Janowski, B. A.; Corey, D. R. *Chem. Biol.* **2004**, *11*, 749–758.
(10) Nielsen, P. E. *Chem. Biodiversity* **2010**, *7*, 786–804.
(11) Dervan, P. B.; Edelson, B. S. *Curr. Opin. Struct. Biol.* **2003**, *13*, 284–299.
(12) Kutyavin, I. V.; Rhinehart, R. L.; Lukhtanov, E. A.; Gorn, V. V.; Meyer, R. B., Jr.; Gamper, H. B., Jr. *Biochemistry* **1996**, *35*, 11170–11176.
(13) Lohse, J.; Dahl, O.; Nielsen, P. E. *Proc. Natl. Acad. Sci. U.S.A.* **1999**, *96*, 11804–11808.
(14) Ishizuka, T.; Yoshida, J.; Yamamoto, Y.; Sumaoka, J.; Tedeschi, T.; Corradini, R.; Sforza, S.; Komiyama, M. *Nucleic Acids Res.* **2008**, *36*, 1464–1471.
(15) Janowski, B. A.; Kaihatsu, K.; Huffman, K. E.; Schwartz, J. C.; Ram, R.; Hardy, D.; Mendelson, C. R.; Corey, D. R. *Nat. Chem. Biol.* **2005**, *1*, 210–215.
(16) Beane, R.; Gabillet, S.; Montaillier, C.; Arar, K.; Corey, D. R. *Biochemistry* **2008**, *47*, 13147–13149.
(17) Rapireddy, S.; Bahal, R.; Ly, D. H. *Biochemistry* **2011**, *50*, 3913–3918.
(18) Bahal, R.; Sahu, B.; Rapireddy, S.; Lee, C.-M.; Ly, D. H. *ChemBioChem* **2012**, *13*, 56–60.
(19) Rusling, D. A.; Powers, V. E. C.; Ranasinghe, R. T.; Wang, Y.; Osborne, S. D.; Brown, T.; Fox, K. *Nucleic Acids Res.* **2005**, *33*, 3025–3032.
(20) Hari, Y.; Obika, S.; Imanishi, T. *Eur. J. Org. Chem.* **2012**, 2875–2887.
(21) Bogdanove, A. J.; Voytas, D. F. *Science* **2011**, *333*, 1843–1846.
(22) Gaj, T.; Gersbach, C. A.; Barbas, C. F., III. *Trends Biotechnol.* **2013**, *31*, 397–405.
(23) Tse, W. C.; Boger, D. L. *Chem. Biol* **2004**, *11*, 1607–1617.
(24) Hamilton, P. L.; Arya, D. P. *Nat. Prod. Rep.* **2012**, *29*, 134–143.
(25) Bryld, T.; Højland, T. R.; Wengel, J. *Chem. Commun.* **2004**, 1064–1065.
(26) Filichev, V. V.; Vester, B.; Hansen, L. H.; Pedersen, E. B. *Nucleic Acids Res.* **2005**, *33*, 7129–7137.
(27) Ge, R.; Heinonen, J. E.; Svahn, M. G.; Mohamed, A. J.; Lundin, K. E.; Smith, C. I. E. *FASEB J.* **2007**, *21*, 1902–1914.
(28) Moreno, P. M. D.; Geny, S.; Pabon, Y. V.; Bergquist, H.; Zaghloul, E. M.; Rocha, C. S. J.; Oprea, I. I.; Bestas, B.; Andaloussi, S. E. L.; Jørgensen, P. T.; Pedersen, E. B.; Lundin, K. E.; Zain, R.; Wengel, J.; Smith, C. I. E. *Nucleic Acids Res.* **2013**, *41*, 3257–3273.
(29) Hrdlicka, P. J.; Kumar, T. S.; Wengel, J. *Chem. Commun.* **2005**, 4279–4281.
(30) The following nomenclature describes the relative arrangement between two monomers positioned on opposing strands in a duplex. The number *n* describes the distance measured in number of base pairs and has a positive value if a monomer is shifted toward the 5′-side of its own strand relative to a second reference monomer on the other strand or a negative value if a monomer is shifted toward the 3′-side of its own strand relative to a second reference monomer on the other strand.
(31) Sau, S. P.; Kumar, T. S.; Hrdlicka, P. J. *Org. Biomol. Chem.* **2010**, *8*, 2028–2036.

(32) Kumar, T. S.; Madsen, A. S.; Østergaard, M. E.; Sau, S. P.; Wengel, J.; Hrdlicka, P. *J. Org. Chem.* **2009**, *74*, 1070−1081.
(33) Nielsen, C. B.; Petersen, M.; Pedersen, E. B.; Hansen, P. E.; Christensen, U. B. *Bioconjugate Chem.* **2004**, *15*, 260−269.
(34) Karmakar, S.; Anderson, B. A.; Rathje, R. L.; Andersen, S.; Jensen, T.; Nielsen, P.; Hrdlicka, P. J. *J. Org. Chem.* **2011**, *76*, 7119−7131.
(35) Kalra, N.; Babu, B. R.; Parmar, V. S.; Wengel, J. *Org. Biomol. Chem.* **2004**, *2*, 2885−2887.
(36) Nakamura, M.; Fukunaga, Y.; Sasa, K.; Ohtoshi, Y.; Kanaori, K.; Hayashi, H.; Nakano, H.; Yamana, K. *Nucleic Acids Res.* **2005**, *33*, 5887−5895.
(37) Didion, B. A.; Karmakar, S.; Guenther, D. C.; Sau, S. P.; Verstegen, J. P.; Hrdlicka, P. J. *ChemBioChem* **2013**, *4*, 3447−3454.
(38) Denn, B.; Karmakar, S.; Guenther, D. C.; Hrdlicka, P. J. *Chem. Commun.* DOI: 10.1039/C3CC45705B.
(39) Kumar, T. S.; Madsen, A. S.; Wengel, J.; Hrdlicka, P. J. *J. Org. Chem.* **2006**, *71*, 4188−4201.
(40) (a) Andersen, N. K.; Wengel, J.; Hrdlicka, P. J. *Nucleosides, Nucleotides Nucleic Acids* **2007**, *26*, 1415−1417. (b) The synthesis of monomer **M** will be published elsewhere.
(41) Winnik, F. M. *Chem. Rev.* **1993**, *93*, 587−614.
(42) Dioubankova, N. N.; Malakhov, A. D.; Stetsenko, D. A.; Gait, M. J.; Volynsky, P. E.; Efremov, R. G.; Korshun, V. A. *ChemBioChem* **2003**, *4*, 841−847.
(43) Astakhova, I. V.; Malakhov, A. D.; Stepanova, I. A.; Ustinov, A. V.; Bondarev, S. L.; Paramonov, A. S.; Korshun, V. A. *Bioconjugate Chem.* **2007**, *18*, 1972−1980.
(44) Astakhova, I. V.; Ustinov, A. V.; Korshun, V. A.; Wengel, J. *Bioconjugate Chem.* **2011**, *22*, 533−539.
(45) Hrdlicka, P. J.; Babu, B. R.; Sørensen, M. D.; Wengel, J. *Chem. Commun.* **2004**, 1478−1479.
(46) Hwang, G. T.; Seo, Y. J.; Kim, B. H. *Tetrahedron Lett.* **2005**, *46*, 1475−1477.
(47) Grünewald, C.; Kwon, T.; Piton, N.; Förster, U.; Wachtveitl, J.; Engels, J. W. *Bioorg. Med. Chem.* **2008**, *16*, 19−26.
(48) Nakamura, M.; Murakami, Y.; Sasa, K.; Hayashi, H.; Yamana, K. *J. Am. Chem. Soc.* **2008**, *130*, 6904−6905.
(49) Astakhova, I. V.; Lindegaard, D.; Korshun, V. A.; Wengel, J. *Chem. Commun.* **2010**, *46*, 8362−8364.
(50) Seela, F.; Ingale, S. A. *J. Org. Chem.* **2010**, *75*, 284−295.
(51) Ingale, S. A.; Pujari, S. S.; Sirivolu, V. R.; Ding, P.; Xiong, H.; Mei, H.; Seela, F. *J. Org. Chem.* **2012**, *77*, 188−199.
(52) Kumar, P. K.; Shaikh, K. I.; Jørgensen, A. S.; Kumar, S.; Nielsen, P. *J. Org. Chem.* **2012**, *77*, 9562−9573.
(53) Langenegger, S. M.; Häner, R. *Chem. Commun.* **2004**, 2792−2793.
(54) Haner, R.; Garo, F.; Wenger, D.; Malinovskii, V. L. *J. Am. Chem. Soc.* **2010**, *132*, 7466−7471.
(55) Wojciechowski, F.; Lietard, J.; Leumann, C. J. *Org. Lett.* **2012**, *14*, 5176−5179.
(56) Cornell, W. D.; Cieplak, P.; Bayly, C. I.; Gould, I. R.; Merz, K. M.; Ferguson, D. M.; Spellmeyer, D. C.; Fox, T.; Caldwell, J. W.; Kollman, P. A. *J. Am. Chem. Soc.* **1995**, *117*, 5179−5197.
(57) Pérez, A.; Marchán, I.; Svozil, D.; Sponer, J.; Cheatham, T. E.; Laughton, C. A.; Orozco, M. *Biophys. J.* **2007**, *92*, 3817−3829.
(58) Still, W. C.; Tempczyk, A.; Hawley, R. C.; Hendrickson, T. *J. Am. Chem. Soc.* **1990**, *112*, 6127−6129.
(59) *MacroModel*, version 9.8; Schrödinger, LLC: New York, 2010.
(60) Crothers, D. M. *Biopolymers* **1968**, *6*, 575−584.
(61) For additional validation of this assay, see ref 37.
(62) Wadkins, R. M. *Curr. Med. Chem.* **2000**, *7*, 1−15.
(63) Keene, F. R.; Smith, J. A.; Collins, J. G. *Coord. Chem. Rev.* **2009**, *253*, 2021−2035.
(64) Nakamura, M.; Shimomura, Y.; Ohtoshi, Y.; Sasa, K.; Hayashi, H.; Nakano, H.; Yamana, K. *Org. Biomol. Chem.* **2007**, *5*, 1945−1951.